Cation Exchange Synthesis of Uniform PbSe/PbS Core/Shell Tetrapods and their use as Near-Infrared Photodetectors

Nimai Mishra,[1] * Bablu Mukherjee,[2] Guichuan Xing,[3] Sabyasachi Chakrabortty,[1] Asim Guchhait,[1] and Jessica Yin Lim[1]

[1]Department of Chemistry, National University of Singapore, 3 Science Drive 3, Singapore 117543
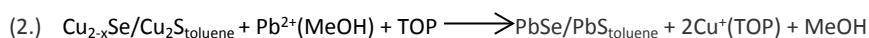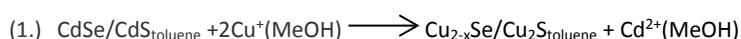[2]Department of Physics, National University of Singapore, 2 Science Drive 3, Singapore 117542
[3]Division of Physics and Applied Physics, School of Physical and Mathematical Sciences, Nanyang Technological University, 21 Nanyang Link, Singapore 637371

Contact: Nimai@lanl.gov

1. Cation exchange synthesis of $Cu_{2-x}Se/Cu_{2-x}S$ and PbSe/PbS tetrapods:

The efficiency of cation exchange reactions depends on the thermodynamic driving force and the activation barrier. In order for the reaction to be thermodynamically favorable, suitable conditions are needed such that the new cations are able to bond well with the anionic framework while the original cations form stable complexes with the complexing agents. The activation barrier for the cation exchange reaction depends on several factors including the ionic interaction between cations and anions, the structure of the anionic framework and the difference between the nanocrystal structures formed by the reactants and products in the reaction. By varying the solvent environment, we can control the cation solvation to some extent. Since each exchange reaction involves two cations, different solvent environments can be used to dissolve the cations precursor while dispersing the original nanocrystal. At the same time, different environments can separate the newly formed cation-exchanged complex from the released original cations after the cation exchange reaction. The simplest way to manipulate the solvation conditions is to vary solvents with different polarities in order to encourage a favorable forward reaction. In the $Cd^{2+} \rightarrow Cu^+ \rightarrow Pb^{2+}$ cation exchange process, the forward reaction was favored by suspending the tetrapods in toluene and dissolving the precursor salt in methanol. These reactions can be understood in terms of the hard-soft acid-base theory.

(1.) $CdSe/CdS_{toluene} + 2Cu^+(MeOH) \longrightarrow Cu_{2-x}Se/Cu_2S_{toluene} + Cd^{2+}(MeOH)$

(2.) $Cu_{2-x}Se/Cu_2S_{toluene} + Pb^{2+}(MeOH) + TOP \longrightarrow PbSe/PbS_{toluene} + 2Cu^+(TOP) + MeOH$

Scheme: $Cd^{2+} \rightarrow Cu^+ \rightarrow Pb^{2+}$ cation reaction process. Subscripts indicate suspension while brackets indicate solvation

During the cation exchange with Cu^+, MeOH acts as a hard base and will preferentially bind to Cd^{2+} cations which are relatively harder metals as compared to Cu^+. At the same time, the Cu^+ cations will replace the Cd^{2+} cations in the anionic framework. In the sequential cation exchange reaction, TOP acts as a soft base to bind to Cu^+ cations while harder Pb^{2+} cations enter the anionic framework. The addition of TOP provides a driving force for this cation exchange reaction since experiments performed without the addition of TOP resulted in unsuccessful cation exchange reactions in order to obtain PbSe/PbS tetrapods.
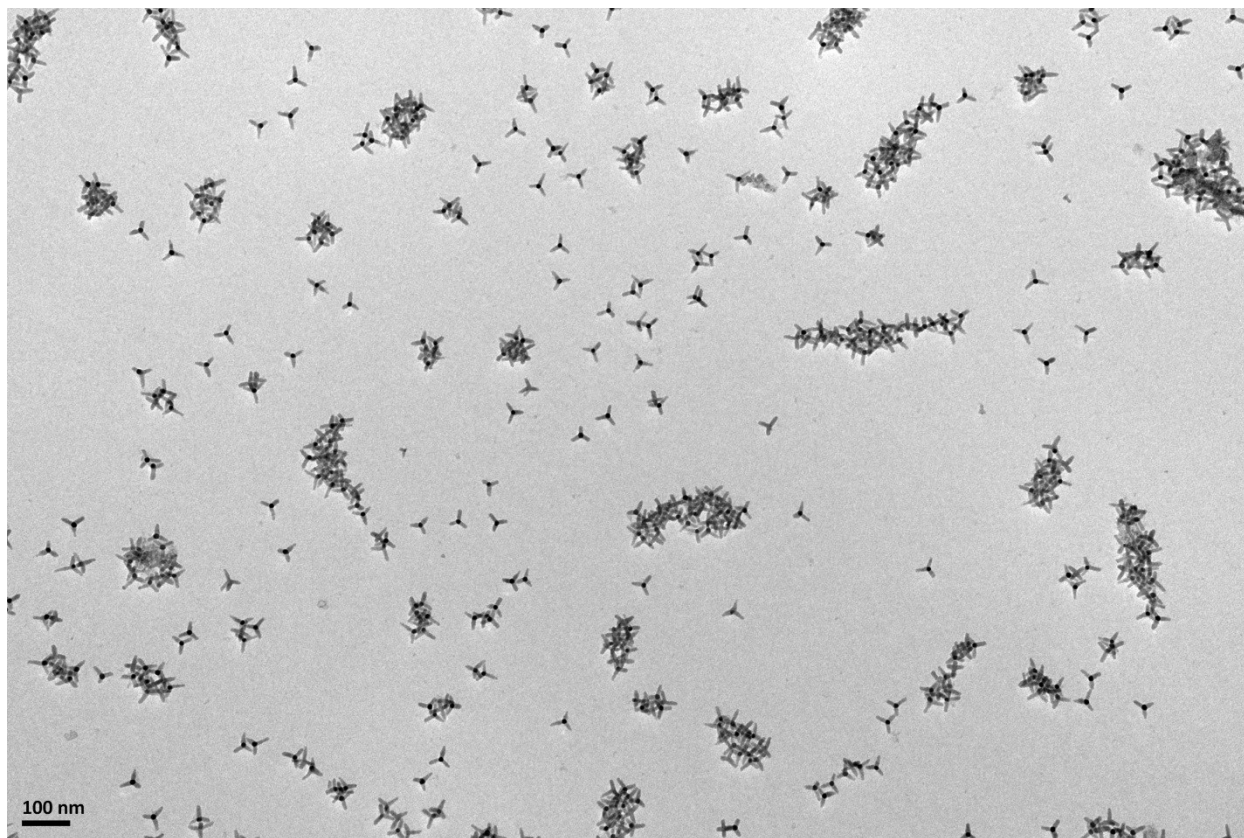
2. Large view TEM image of PbSe/PbS tetrapods:

Figure S1. A large scale view of a low resolution TEM image of as-synthesized PbSe seeded PbS tetrapods. From typical sample sizes of ~500 particles, we deduced that the yield of tetrapods for this synthetic strategy generally ranged from 90-95 % on average.

3. Large view TEM image of Cu$_{2-x}$Se/Cu$_2$S tetrapods:

100 nm

Figure S2. A large scale view of a low resolution TEM image of as-synthesized Cu$_{2-x}$Se seeded Cu$_{2-x}$S tetrapods. From typical sample sizes of ~500 particles, we deduced that the yield of tetrapods for this synthetic strategy generally ranged from 90-95% on average.

4. EDX analysis of $Cu_{2-x}Se/Cu_{2-x}S$ tetrapods:

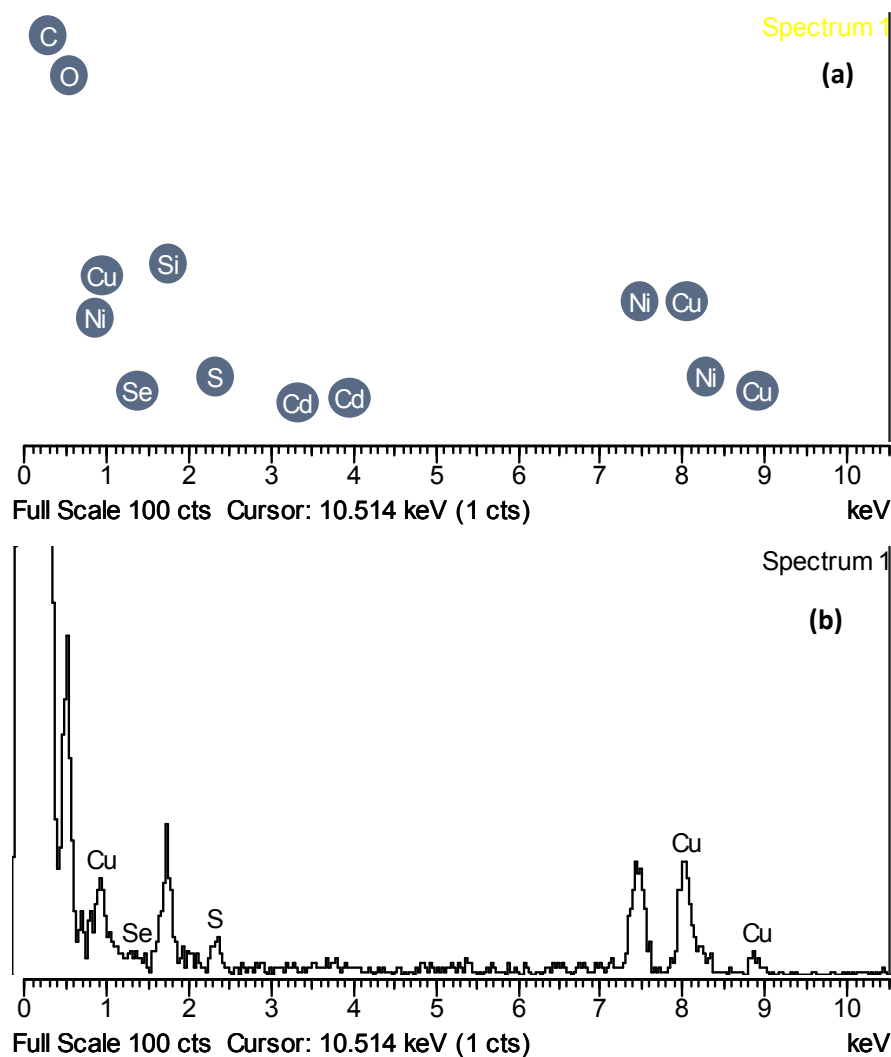**Figure S3**: EDX Spectrum for $Cu_{2-x}Se/Cu_{2-x}S$ tetrapods after cation exchange reaction (a) with all peaks assigned (b) without assigned peaks from nickel grid and low signal impurities.

The EDX spectrum in Figure S3 confirms the formation of $Cu_{2-x}Se/Cu_{2-x}S$ tetrapods after cation exchange. Figure S3(a) shows all the peaks assigned to every element found in the sample and on the carbon coated nickel grid. Figure S3(b) shows the peaks assigned only to copper, sulfur and selenium for easier visualization. The spectra shows that complete cation exchange from CdSe/CdS tetrapods to $Cu_{2-x}Se/Cu_{2-x}S$ tetrapods was successful since the presence of cadmium detected is negligible as compared to the copper, sulfur and selenium signals obtained. This suggests that there is an absence of cadmium cations in the cation-exchanged tetrapods. Low signals of cadmium detected may be due to impurities from leftover cadmium cations that were left behind in the solvent after the $Cu_{2-x}Se/Cu_{2-x}S$ tetrapods have been purified.

5. XRD of Cu$_{2-xSe}$/Cu$_{2-x}$S tetrapods:

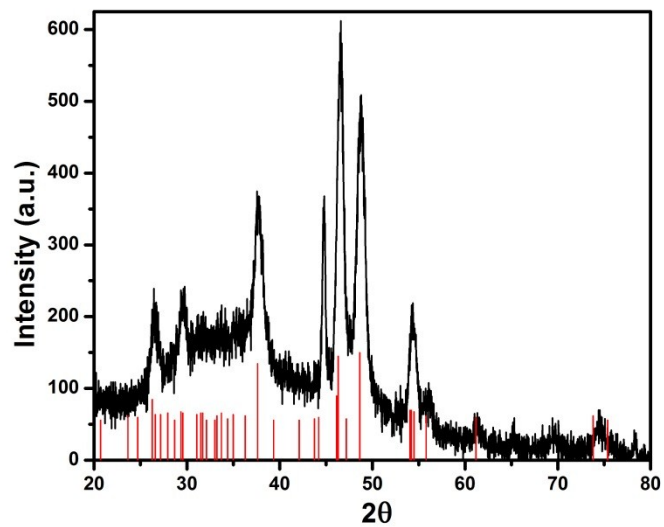**Figure S4**: XRD patterns for Cu$_{2-xSe}$/Cu$_{2-x}$S tetrapods. Which matches with reported JCPDS file no:00-023-0959 with crystals structures of Djurleite and composition of Cu$_{1.94}$S.

6. EDX elemental analysis of the amount of left over Cu in PbSe/PbS tetrapods.
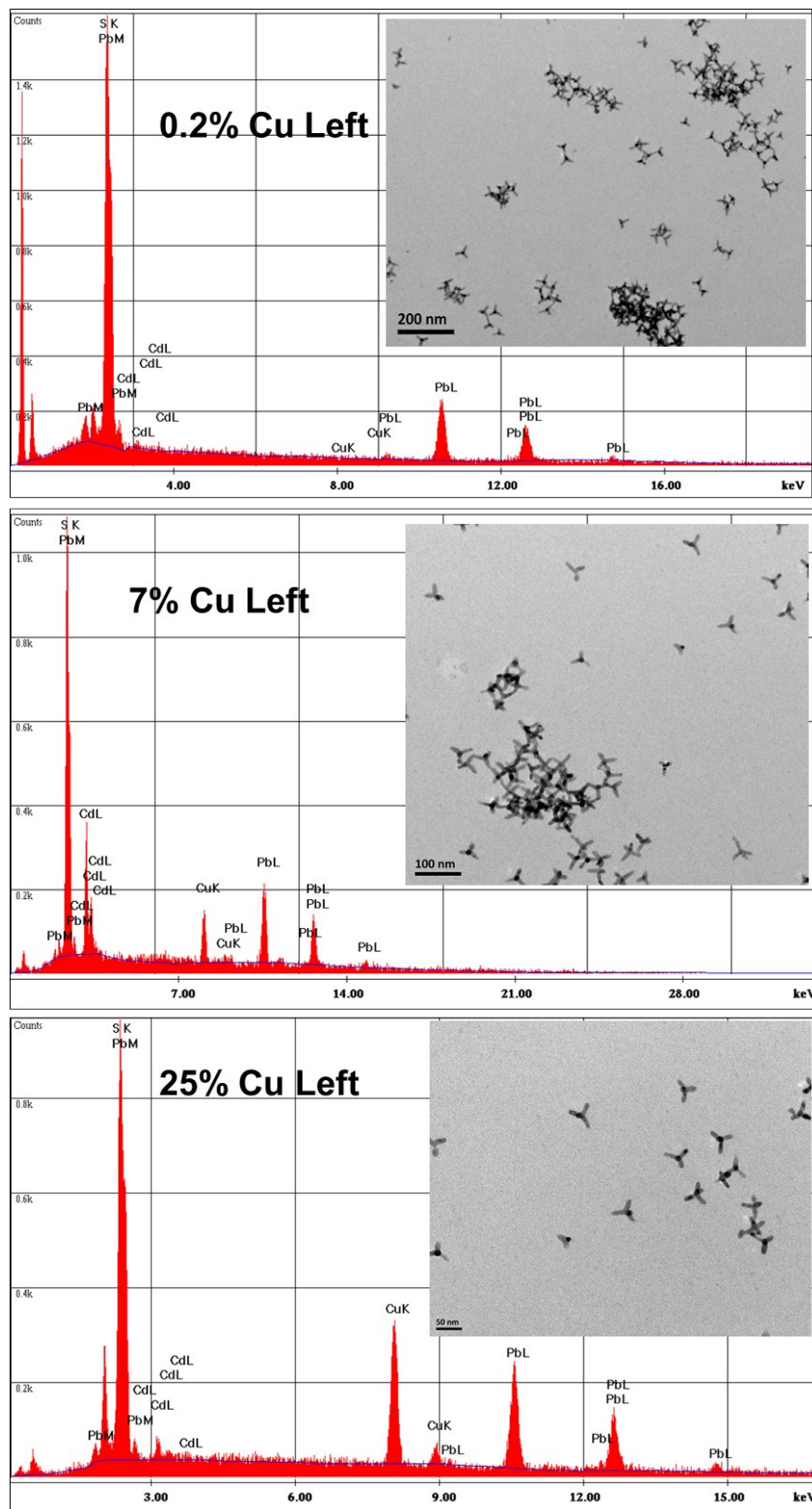

Figure S5: EDX elemental analysis and quantification of elements on three PbSe/PbS tetrapods sample. The % (0.2-25) of Cu left in final product is mentioned in respective EDX data.

7. Fourier transform infrared spectroscopy (FTIR) characterization of surface capping groups on PbSe/PbS tetrapods.
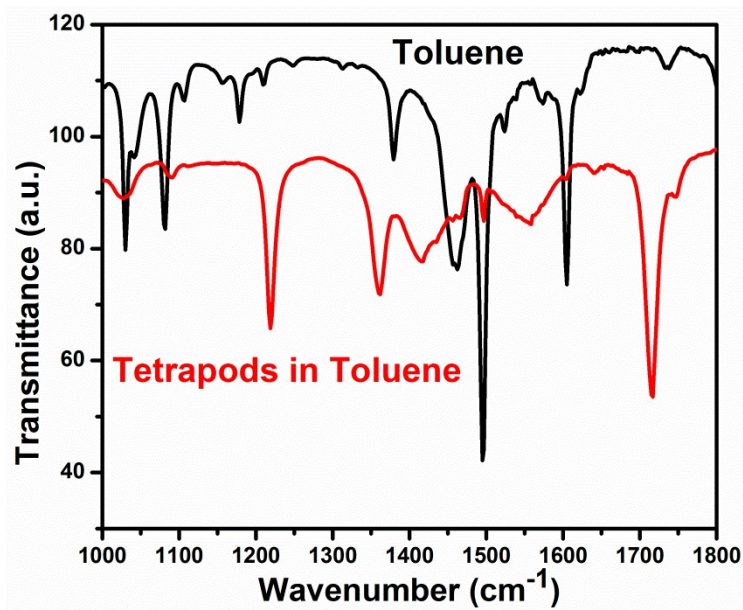

Figure S6: FTIR spectra of the pure toluene (black) and nanocrystals dispersed in toluene (red). Carbonyl stretching vibration of oleic acid was to be found at 1715 cm-1. The results indicate that oleate ligands attached to PbSe-PbS nanocrystals. Phosphonate stretching vibration of the phosphonic acids was to found at 1219 cm-1, which indicates the presence of these ligands on to the PbS surface of the PbSe/PbS tetrapods.